Thermal behaviour, sulfonation and catalytic activity of phenylene-bridged periodic mesoporous organosilicas†

Dolores Esquivel, César Jiménez-Sanchidrián and Francisco J. Romero-Salguero*

Received 7th September 2010, Accepted 7th October 2010
DOI: 10.1039/c0jm02980g

The structural and surface changes in a phenylene-bridged periodic mesoporous organosilica after thermal treatment under different conditions are reported. Organic moieties in the pore walls are stable at temperatures close to 500 °C but calcination in the presence of oxygen leads to C–Si bond cleavage as well as the formation of oxidized groups of phenolic and carbonyl type. The oxidized materials are functionalized by reaction with chlorosulfonic acid in a higher extension than those calcined under nitrogen but all of them preserve their structure and surface properties. All sulfonated organosilicas were active as catalysts for the esterification of acetic acid with ethanol, particularly those calcined in the air. Remarkably, some of them can be even more active than Amberlyst-15 when water is used as reaction medium which is of a high interest for the design of sustainable acid-catalyzed chemical processes.

Introduction

The development of inorganic mesoporous materials of the M41S family was the starting point for the synthesis of a huge number of materials with long-range structural order, very high surface areas and well-defined pore systems, most of them obtained by surfactant-templated methods.[1,2] Later, in order to extend their applications as catalysts, adsorbents and sensors, among others, they were modified by the incorporation of organic fragments. In general, this was accomplished by either post-synthesis treatment[3,4] (grafting) or co-condensation.[5,6] The former involved the use of organotrialkoxysilanes bearing terminal organic groups, $(R'O)_3Si–R$, which were anchored to the surface of a preformed mesoporous silica whereas the latter was based on the condensation of both tetraalkoxysilanes, typically $Si(OEt)_4$ or $Si(OMe)_4$, and organotrialkoxysilanes in the presence of the structure-directing agent. More recently, three research groups reported the synthesis of new hybrid organic–inorganic materials, the so-called PMOs (periodic mesoporous organosilicas).[7–9] They were synthesized from bridged organosilanes of the type $(R'O)_3–Si–(O'R)_3$ in the presence of a surfactant giving rise to well-ordered mesoporous structures with a homogeneous distribution of organic fragments. Currently, numerous PMO materials with different organic moieties have been described, such as those containing methylene,[10–12] ethylene,[8,12,13] ethylidene,[7,14–16] phenylene,[17–22] biphenylene,[23,24] thiophene[17,25,26] and anthracene[27–29] groups.

Among PMO materials, those incorporating benzene bridges have attracted a great interest. Since Ozin *et al.*[17] carried out their first synthesis under acidic conditions by using CPCl (cetylpiridinium chloride) as surfactant, other analogous materials have been prepared under a variety of conditions. Thus, a broad range of materials with different structural (pore sizes,[17,19] dimensionality of the channel system,[30–32] crystal-like walls,[18,33–37]…) and morphological (spherical particles,[38] monoliths,[39] thin films,[40–43]…) features have been obtained.

Recently, several sulfonic acid functionalized PMOs have been synthesized as a new class of acid catalysts. They combine their high surface area and good accessibility to the active sites with the increased hydrophobicity of their pore walls. Inagaki *et al.*[18] reported the direct sulfonation of the phenyl rings in the first PMOs with periodic pore walls although its catalytic activity was not tested. Kapoor *et al.*[31,32] showed that sulfuric acid functionalized phenylene-bridged PMOs with a cubic structure (*Pm3n*) obtained by a post-synthesis process with different sulfonating agents were highly active in the Friedel–Crafts acylation reaction between anisole and acetic anhydride. Also, either the co-condensation of 1,4-bis(triethoxysilyl)benzene and 3-mercaptopropyltrialkoxysilanes or the grafting of the latter on the preformed PMOs, and the subsequent oxidation of the thiol (–SH) to sulfonic acid ($–SO_3H$) groups provided PMOs with high acidity which have been used as catalysts for condensation, esterification and hydration.[44–51] Their increased activity and stability have been related to the large amount of propyl–SO_3H groups anchored in the pore walls together with the hydrophobicity of the organic moieties which improves their catalytic results in organic reactions, such as esterification, where the presence of water is unavoidable. A different strategy has been also used for functionalizing ethylidene-bridged PMOs, which consisted in the previous introduction of a phenyl ring. Thus, Kondo *et al.*[52] reported its Diels–Alder reaction with benzocyclobutene whereas Kaliaguine *et al.*[53] investigated its alkylation with benzene. In both cases, the resulting aromatic ring was sulfonated.

Herein we report the structural and surface modifications which have taken place in a phenylene-bridged PMO, prepared from 1,4-bis(triethoxysilyl)benzene and Brij 76 as structure-directing agent, after calcination under different conditions. The resulting materials have been reacted with chlorosulfonic acid,

Department of Organic Chemistry, Faculty of Sciences, University of Córdoba, Campus de Rabanales, Marie Curie Building, Ctra. Nnal. IV, km 396, 14071 Córdoba, Spain. E-mail: qo2rosaf@uco.es; Fax: +34 957212066; Tel: +34 957212065

† Electronic supplementary information (ESI) available: Initial sulfonation tests with different agents, ^{13}C and ^{29}Si NMR spectra and N_2 isotherms of sulfonated samples. See DOI: 10.1039/c0jm02980g

thus giving different sulfonic acid functionalized phenylene-bridged PMOs, which have been used as acid catalysts for the esterification of acetic acid with ethanol.

Experimental section

Chemicals

The phenylene-bridged PMO was synthesized using the 1,4-bis(triethoxysilyl)benzene (BTEB) (96%, Aldrich) as the organosilica precursor. Brij 76 (polyoxyethylene(10)stearyl alcohol) (Aldrich) was used as the structure directing agent and HCl (35% w/v, Panreac) as an acid source. The surfactant was removed by successive acidized ethanol extractions. Chlorosulfonic acid (99%, Aldrich) was used to functionalize the PMOs. Acetic acid (Aldrich) and ethanol (Panreac) were used as reactants in the catalytic activity tests.

Synthesis

The parent phenylene-bridged mesoporous material was synthesized according to the procedure reported by Burleigh *et al.*[16] Typically, 6 g of Brij 76 surfactant were dissolved in a solution of 19.6 ml HCl and 279 ml H_2O followed by stirring at 50 °C for 24 h. After adding 15.9 ml organosilane, the mixture was stirred for 24 h at the same temperature. The resulting gel was then aged at 90 °C for 24 h under static conditions. A white powder was collected by filtration and thoroughly washed with H_2O. In order to remove the surfactant, 1 g of as-synthesized material was stirred in a solution of 1 ml HCl in 50 ml ethanol for 12 h at 80 °C. After repeating this process twice, the solid product was recovered by filtration, washed with ethanol and dried under vacuum for 10 h.

Thermal treatments

The surfactant-extracted material (named as Ph) was subjected to several thermal conditions, giving rise to different materials, which are listed in Table 1.

Sulfonation of Ph–PMOs

In general, sulfonic acid groups were introduced in the Ph–PMO materials after thermal treatment by reaction with chlorosulfonic acid. It was chosen as the sulfonating agent because previous tests indicated that both concentrated and fuming sulfuric acids led to structural degradation of the organosilica framework (see Table S1, ESI†). All solids were heated at 140 °C under vacuum for 3 h. Sulfonation was carried out as follows: a solution of 30 ml CH_2Cl_2 and 0.35 ml $ClSO_3H$ was stirred at 0 °C for 30 min. Later, 0.2 g Ph–PMOs were added and the mixture was stirred at 0 °C for 4 h.[54] After warming to room temperature, the mixture was filtered and the solid was added to 500 ml of deionized water. This suspension was stirred at 70 °C for 2 h to remove residual sulfuric acid. This process was repeated twice. After filtration, the solid was washed with abundant water until it became neutral. Finally, the sulfonated Ph–PMOs were dried at 120 °C under vacuum.

Table 1 Nomenclature of the phenylene-bridged PMO materials (Ph-PMOs) subjected to different thermal treatments

Name	T/°C	Atmosphere	Duration/h
Ph–N_2	400	Nitrogen flow[a]	8
Ph–N_2 : H_2O	400	Nitrogen flow saturated with H_2O[a]	8
Ph-air	400	Air flow[a]	8
Ph-air : H_2O	400	Air flow saturated with H_2O[a]	8
Ph-air (oven)	400	Air (oven)	15
Ph-air (600 °C)	600	Air (oven)	15
Ph-air (800 °C)	800	Air (oven)	15

[a] Both nitrogen and air flows at 14 ml s^{-1}.

Catalytic reaction

The catalytic activity of the sulfonic acid functionalized PMOs was studied in the esterification of acetic acid with ethanol, and compared with that of Amberlyst-15 as a reference. The reaction was carried out in a two-necked round-bottomed flask equipped with a reflux condenser and a magnetic stir bar. The catalyst (0.150 g) was pretreated at 120 °C overnight under vacuum before the catalytic reaction and then added to a mixture of acetic acid (0.076 mol) and ethanol (0.760 mol). The esterification reaction was carried out under refluxing at 70 °C in a N_2 atmosphere. Samples collected at regular intervals were analysed by gas chromatography, using a HP-1 30 m × 0.5 mm ID methyl silicone capillary column and a constant temperature programme at 50 °C. Reaction products were identified by the use of standards and quantified with dioxane as internal standard by using a FID detector.

Characterization

X-Ray powder diffraction (XRD) patterns were recorded on a Siemens D-5000 powder diffractometer (Cu-Kα radiation). N_2 isotherms were determined on a Micromeritics ASAP 2010 analyzer at −196 °C. The specific surface area of each solid was determined using the BET method over a relative pressure (P/P_0) range of 0.05–0.30. Prior to measurement, the samples were outgassed at 403 K for 24 h. The pore size distribution was obtained by analysis of the desorption branch of the isotherms using the Barrett–Joyner–Halenda (BJH) method. The ^{29}Si and ^{13}C MAS NMR spectra were recorded at 79.49 MHz and 100.61 MHz, respectively, on a Bruker ACP-400 spectrometer at room temperature. An overall 1000 free induction decays were accumulated. The excitation pulse and recycle time for ^{29}Si MAS NMR were 6 μs and 60 s, respectively, and those for ^{13}C MAS NMR spectra 6 μs and 2 s. Chemical shifts were measured relative to a tetramethylsilane standard. Prior to measurement, samples were dehydrated in a stove at 423 K for 24 h. Deconvolution of the ^{29}Si MAS NMR spectra was performed with DM2006 software. The structural condensation degree was calculated according to the general formula $D = [\sum(nT_n) + \sum(nQ_n)]/[(3 \times \sum T_n) + (4 \times \sum Q_n)]$ that represents the ratio between the number of Si–O–Si linkages existing in the material and the number of Si–O–Si linkages which could be obtained if the network condensation would be at the maximum. UV-vis spectra were recorded on an UV-Visible Diffuse Reflectance Spectrophotometer Varian Carey IE. The diffuse reflectance infrared Fourier transform (DRIFT) spectra of the samples were

collected on a Perkin-Elmer 2000 FTIR spectrometer. The powder sample was placed in a diffuse reflectance environmental chamber (Harrick) connected to a temperature controller. The sample was heated *in situ* from room temperature to 400 °C under nitrogen. Simultaneous thermogravimetric analysis (TGA) and differential thermal analysis (DTA) were performed using a thermobalance Setaram Setsys 12 under an air flow (40 ml min^{-1}) heating at 10 °C min^{-1} from room temperature up to 1000 °C. Raman spectra were acquired with a Renishaw Raman in Via spectrometer equipped with a Leika DM LM microscope and a 785 nm HPNIR diode laser as an excitation source. An acquisition time of 60 s was used for each spectrum at 100% laser power.

Results and discussion

The XRD pattern of the parent organosilica Ph–PMO exhibited a low angle (100) peak with a *d*-spacing of 55.1 Å and broad and short second-order (110) and (200) peaks at higher incidence angles indicative of materials with 2D hexagonal (*P6mm*) mesopore structures (Fig. 1). The extraction with an acidified ethanolic solution to ensure removal of the surfactant did not change much the *d*-spacing but slightly increased the intensity of the (110) and (200) diffractions. However, the low angle (100) peak was shifted to a higher angle upon calcination whatever the conditions, thus indicating a gradual unit cell contraction, particularly in the Ph-air : H_2O sample (Table 2). This effect was more remarkable at 600 and 800 °C (Fig. 1). In the last case, the (100) peak was very broad, thus evidencing a more disordered mesostructure in such material.

Table 2 Physicochemical properties of periodic mesoporous materials

Sample	d^a/Å	BET surface area/m^2 g^{-1}	Total pore volume/cm^3 g^{-1}	Pore size^b/Å	Wall thickness^c/Å
Ph	55	977	0.70	35	28
Ph–N_2	52	969	0.71	32	28
Ph–N_2 : H_2O	51	910	0.67	—	—
Ph-air	51	907	0.66	30	29
Ph-air (oven)	51	905	0.59	28	31
Ph-air : H_2O	49	771	0.44	26	31

[a] *d*(100) spacing of the materials from XRD. [b] Calculated from the desorption branch. [c] Estimated from (a_0—pore size), where $a_0 = (2d_{100}/\sqrt{3})$.

The N_2 adsorption–desorption isotherm for the Ph sample was of type IV with the step at a relative pressure around 0.4 (*i.e.* typical of mesoporous solids) (Fig. 2). The average pore diameter and the narrow pore size distribution confirmed the presence of pores in the mesopore range (Fig. 3). Once calcined, the resulting materials exhibited similar isotherms but slightly smaller pore sizes and pore volumes. The surface areas were around 900 m^2 g^{-1}, except for the Ph-air : H_2O sample which had less than 800 m^2 g^{-1}. This material showed a slightly broader low angle (100) peak and negligible high order diffractions indicative of a lower structural quality than the other Ph–PMOs.

The thermogravimetric analysis of the as-synthesized Ph–PMO material under air exhibited four main weight losses (Fig. 4). The first, below 120 °C and associated to an endothermic peak, was related to the loss of water and ethanol adsorbed on the surface of this sample. The second was centered at *ca.* 250 °C and would correspond to the decomposition of the surfactant in the mesopores. A third small loss at about 400 °C might be assigned to the decomposition of ethoxide groups ($SiOC_2H_5$). Finally, the phenylene bridges were removed from the structure in the range 500–700 °C, thus revealing the relatively high thermal stability of this kind of materials. The last three losses were associated to decomposition of organic matter and therefore to exothermic peaks. Of course, after the extraction of the surfactant only a very small weight loss still remained at 250 °C, besides those above 400 °C. As expected, once the Ph material was calcined in air, the only observable weight loss occurred at 600 °C due to the decomposition of the phenylene bridges. According to the TGA curve, it accounted for *ca.* 30%, whereas the theoretical weight loss for the hybrid solid ($Si_2O_3C_6H_4$) is 42%. This difference was probably due to the deviation of the actual composition relative to the theoretical one (it would correspond to a fully condensed silica, which is not the case as demonstrated below by ^{29}Si MAS NMR) as well as the existence of residual carbon fragments in the resulting solids.

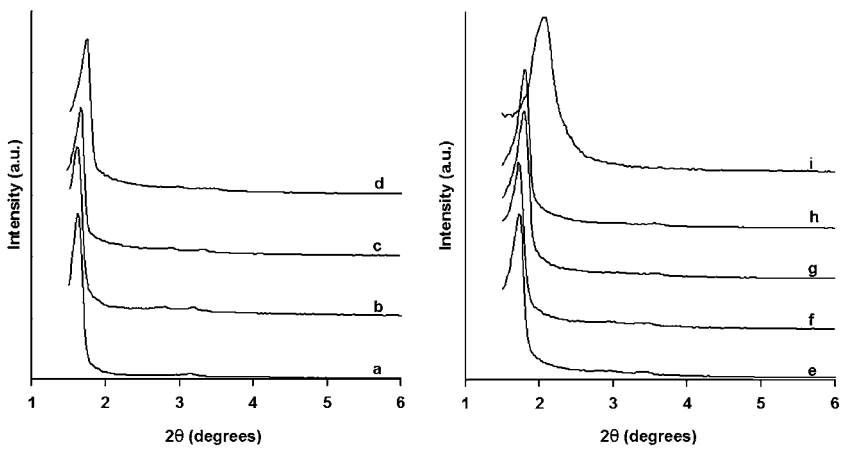

Fig. 1 X-Ray diffraction patterns of phenylene-bridged periodic mesoporous organosilicas: (a) as-synthesized, (b) after surfactant removal (2^{nd} extraction), (c) Ph–N_2, (d) Ph–N_2 : H_2O, (e) Ph-air, (f) Ph-air (oven), (g) Ph-air : H_2O, (h) Ph-air (600 °C), and (i) Ph-air (800 °C).

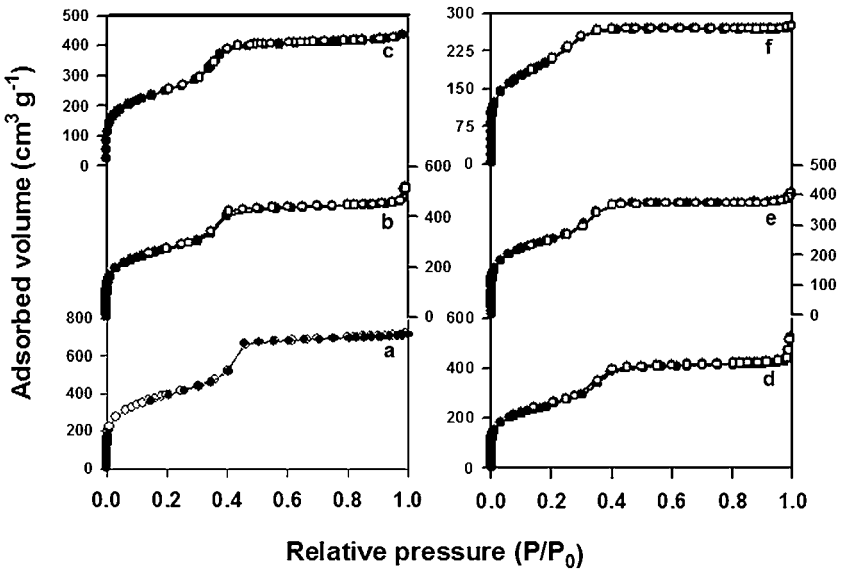

Fig. 2 Nitrogen adsorption–desorption isotherms of phenylene-bridged PMO materials: (a) after surfactant removal (2nd extraction), (b) Ph–N_2, (c) Ph–N_2 : H_2O, (d) Ph-air, (e) Ph-air (oven), and (f) Ph-air : H_2O.

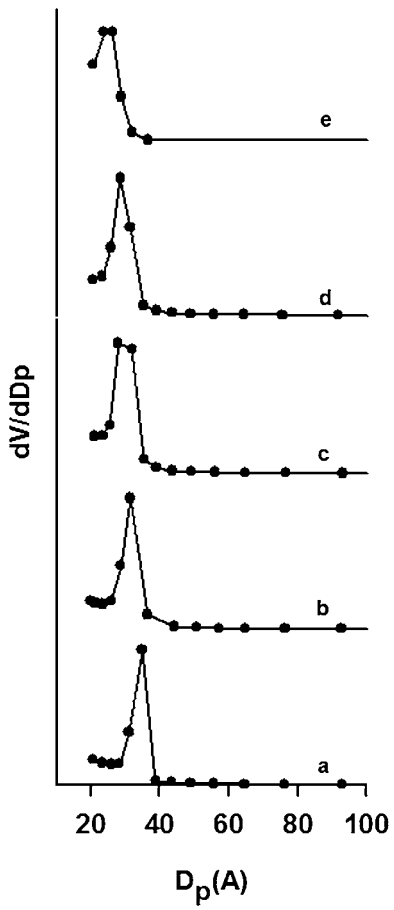

Fig. 3 Pore size distribution curves of the phenylene-bridged PMO materials: (a) after surfactant removal (2nd extraction), (b) Ph–N_2, (c) Ph-air, (d) Ph-air (oven), and (e) Ph-air : H_2O.

Inagaki *et al.*[55] also reported a weight loss in the range 550–800 °C due to phenylene groups.

The DRIFT spectra of the Ph–PMO materials after the thermal treatments are depicted in Fig. 5. Ph–N_2 and Ph–N_2 : H_2O samples (Fig. 5a and b) exhibited several bands in the range 2800–2975 cm^{-1} attributed to C–H stretching vibrations of the surfactant (Brij-76) or even non-hydrolysed ethoxy groups.[56,57] These bands were practically absent in Ph-air (oven), Ph-air and Ph-air : H_2O samples, thus revealing that only the thermal treatments under an oxidizing atmosphere assure the complete elimination of those organic species. The C–H (3060 and 3015 cm^{-1}) and C=C (1604, 1585 and 1500 cm^{-1}) stretching bands confirmed the presence of the benzene bridges in the solid framework.[58] In addition, those materials calcined under air (Fig. 5c–e) showed a peak at 1720 cm^{-1} which can be assigned to C=O stretching vibrations of carbonyl groups formed by oxidative cleavage of the benzene units. After calcining the Ph–PMO parent material in air above the phenyl rings decomposition temperature (*ca.* 500–600 °C), most vibrations from the organic units disappeared, among them were the C=O and aromatic C–H groups. Two peaks at *ca.* 2964 and 2907 cm^{-1} were observed at 600 °C which can be assigned to C–H stretching modes of organic fragments with sp^3 carbon atoms[59] resulting from the decomposition of the phenylene bridges during the calcination. These bands were absent at higher calcination temperatures (800 °C).

Fig. 6 depicts the Raman spectra of some calcined organosilicas. Hoffmann *et al.*[60] reported a broad vibrational spectroscopic study of several PMOs, including the phenylene-bridged material. The Ph–N_2 material exhibited well resolved peaks corresponding to the vibrational modes of the aromatic rings: 1597 cm^{-1} ν (ring), 1205 and 1250 cm^{-1} δ $(C–H)_{i.p}$ (two-fold-degenerated), 1104 cm^{-1} ring breathing, and 634 cm^{-1} δ $(ring)_{i.p}$. Moreover, bands at 1443, 1453 and 1481 cm^{-1} were assigned to methyl and methylene units from ethoxide groups, whose presence was also confirmed by DRIFT and ^{13}C NMR. A wide band

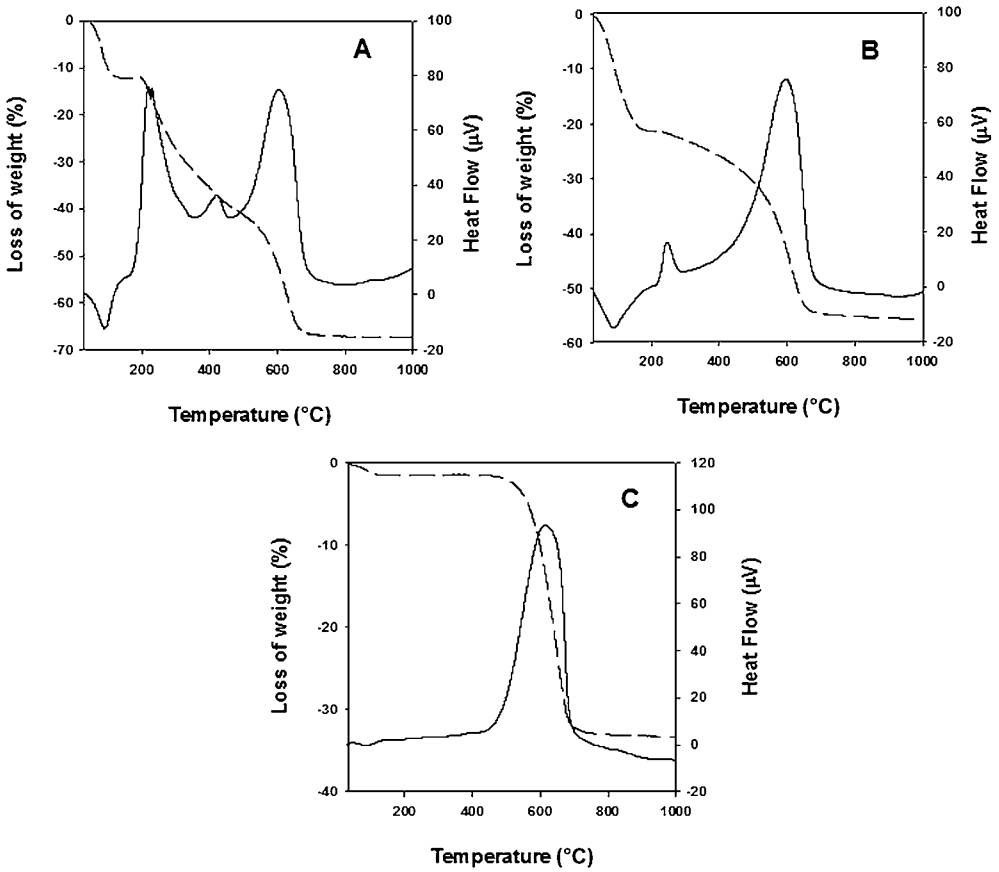

Fig. 4 Thermogravimetric curves (--- TGA) and (— DTA) in air of phenylene-bridged PMOs: (A) as-synthesized, (B) after 2nd extraction and (C) previously calcined in air at 400 °C.

at 584 cm^{-1} could correspond to several deformation δ (Si–O–H) modes. However, the band at *ca.* 780 cm^{-1} could not be assigned yet.[60,61] The Ph-air : H_2O showed broad and ill-defined bands. Both spectra mainly differed in the 1200–1700 cm^{-1} region. Besides ν (ring) and $(C–H)_{i.p}$ vibrations, these bands could tentatively encompass the stretching ν (C=C) and ν (C–C) vibrations at 1660–1694 cm^{-1} and 1328–1410 cm^{-1}, respectively, as expected for quinoid type compounds formed during the calcination process.

UV-vis spectra of as-synthesized and calcined Ph–PMOs are depicted in Fig. 7. They confirmed the presence of the phenylene bridges in most of the samples. The spectra of Ph, Ph–N_2 and Ph–N_2 : H_2O solids exhibited two bands centered at 232 and 272 nm which can be attributed to π–π* electronic transitions characteristic of the benzene rings.[62] All these solids have negligible absorption in the visible region and therefore they are white. However, Ph-air (oven), Ph-air and Ph-air : H_2O materials showed a broad absorption band (from 190 to 500 nm) which can be considered to be composed of the π–π* transitions of the phenylene bridges and a very broad absorption centered at around 420 nm and extended toward the visible region responsible for the yellowish coloration of those materials calcined in the air. The latter must be due to the formation of some chromophores by oxidative cleavage of the phenylene bridges. In accordance with the IR absorption band at 1720 cm^{-1}, they can be tentatively assigned to highly conjugated ketone groups. The color intensity followed the sequence: air : H_2O > air (oven) > air, clearly related to the intensity and broadening of the band at *ca.* 420 nm in the UV-Vis spectra. As shown in Fig. 7, when the Ph material was calcined in the air at 600 or 800 °C, all absorption bands associated to organic groups disappeared, being both spectra similar to that of a pure silica material.

The ^{13}C CP/MAS NMR spectra of the extracted and calcined (up to 400 °C) PMO materials confirmed the presence of phenylene bridges (Fig. 8). All of them possessed a peak centered at 134 ppm corresponding to the overlap of the carbon signals in the phenylene bridges,[16,55] similar to that found in the bis-(triethoxysilyl)benzene spectrum (see Fig. S1†). After two extractions with ethanolic HCl, the Ph sample exhibited two signals at 30 and 70 ppm which are characteristic of the surfactant chain, thus confirming the DRIFT results. Two more signals at 16 and 58 ppm can be assigned to ethoxy groups (Si–O–C_2H_5) which were not completely hydrolyzed under the synthesis conditions. All these signals were not observed in the calcined materials, except for the Ph–N_2 sample where the ethoxy groups still remained. For all calcined materials, the aromatic signal had a shoulder at 128.5 ppm, whose intensity followed the order: Ph-air : H_2O > Ph-air (oven) ≈ Ph-air > Ph–N_2 : H_2O > Ph–N_2. This signal can be associated to Si–Ph groups formed by the cleavage of Si–C bonds. To confirm it, the spectrum of phenyltriethoxysilane was recorded under the same conditions, giving four peaks in the aromatic region at 134.5 (C-2 and C-6), 131

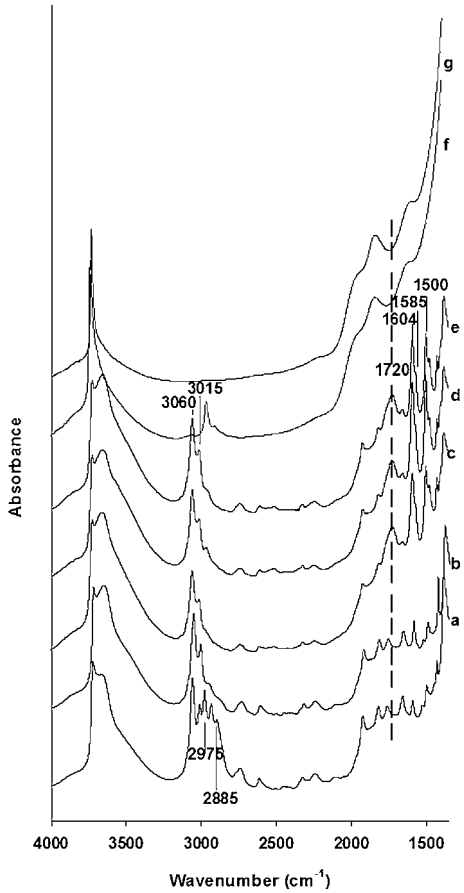

Fig. 5 DRIFT spectra of Ph–PMOs after different thermal treatments: (a) Ph–N_2, (b) Ph–N_2 : H_2O, (c) Ph-air (oven), (d) Ph-air, (e) Ph-air : H_2O and calcined in air (f) at 600 °C and (g) 800 °C.

(C-1), 129 (C-4) and 127 ppm (C-3 and C-5).[63] Thus, that shoulder would encompass these last two signals (see Fig. S2†). Moreover, apart from the previous signals, some solids calcined in the air (*i.e.*, Ph-air : H_2O) exhibited two more shoulders at 122 and 114 ppm as well as a small peak at 154 ppm. We tentatively assign them to phenolic groups (Si–PhOH) resulting from the oxidation of the phenylene bridges. Theoretical chemical shifts for this group are around 157.4, 134.5, 124.1 and 115.8 ppm, which are quite close to those reported for our oxidized Ph–PMOs materials.[64] Kuroki *et al.*[63] reported the existence of two signals at 122 and 152 ppm in the ^{13}C CP/MAS NMR spectra of PMOs prepared from 1,3,5-tris(triethoxysilyl)benzene after a thermal treatment under an oxidizing atmosphere. They tentatively assigned them to oxidized phenyl groups (O–Ph).

The ^{29}Si MAS NMR spectrum of the extracted PMO (Ph sample) exhibited three signals centered at −61.8, −70.5 and −79.6 ppm, that can be assigned to the T^1 [***Si***$C(OH/OEt)_2(OSi)$], T^2 [***Si***$C(OH/OEt)(OSi)_2$] and T^3 [***Si***$C(OSi)_3$] sites, respectively, of the framework (see Fig. S3†). No signals corresponding to SiO_4 species (Q^n sites with n = 1–4, *i.e.* a Si atom attached to four oxygen atoms) were detected, thus precluding the cleavage of C–Si bonds during its synthesis.[16,17,55] However, these signals were observable in the calcined PMOs at *ca.* −91 ppm, −101 ppm and −109 ppm, which can be ascribed to Q^2 [$(SiO)_2Si(OH)_2$], Q^3 [$(SiO)_3SiOH$] and Q^4 [$(SiO)_4Si$] units, respectively. The proportion of Q sites and therefore the amount of cleaved C–Si bonds increased in the order: Ph–N_2 < Ph–N_2 : H_2O (12.8%) < Ph-air (33.30%) < Ph-air (oven) (42.3%) < Ph-air : H_2O (62.4%), being practically absent for the former sample (Table 3). Thus, whereas the Ph–N_2 : H_2O sample preserved a 86% of C–Si bonds after the thermal treatment, the Ph-air : H_2O sample maintained a 40% of these bonds. When a C–Si bond was broken during the thermal treatment, a phenylene bridge formed by both a T^n and a T^m site was transformed into a phenyl silane unit (T^n site) and a silanol group (Q^m site), as shown in Scheme 1. By comparing the T^n to T^m and the T^n to Q^m ratios between Ph–N_2 and the rest of the samples, it seems that the main transformations are T^2–Ph–T^3 to T^3–Ph and Q^2 as well as T^2–Ph–T^2 to T^2–Ph and Q^2. However, as would be expected, in relative terms the most external T sites

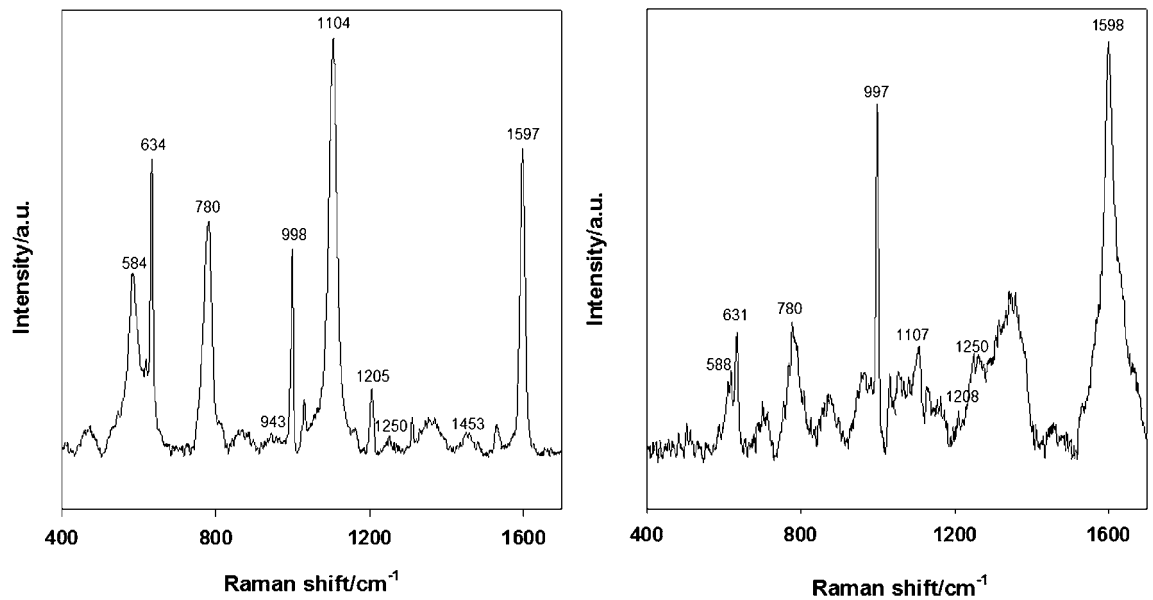

Fig. 6 Raman spectra of Ph–N_2 (left) and Ph-air : H_2O (right) materials.

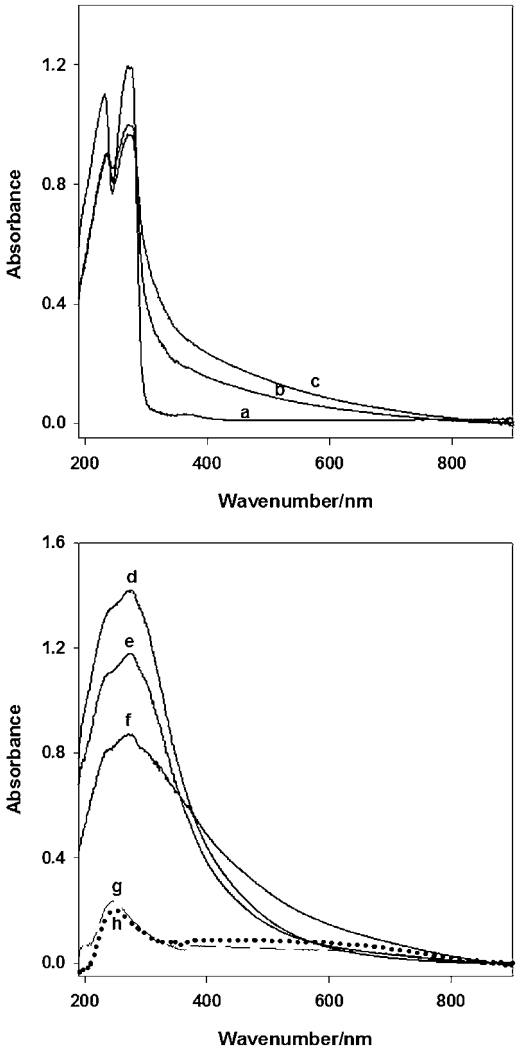

Fig. 7 UV-vis of PMOs materials: (a) Ph, (b) Ph–N_2, (c) Ph–N_2 : H_2O, (d) Ph-air (oven), (e) Ph-air, (f) Ph-air : H_2O and calcined in air (g) at 600 °C and (h) 800 °C.

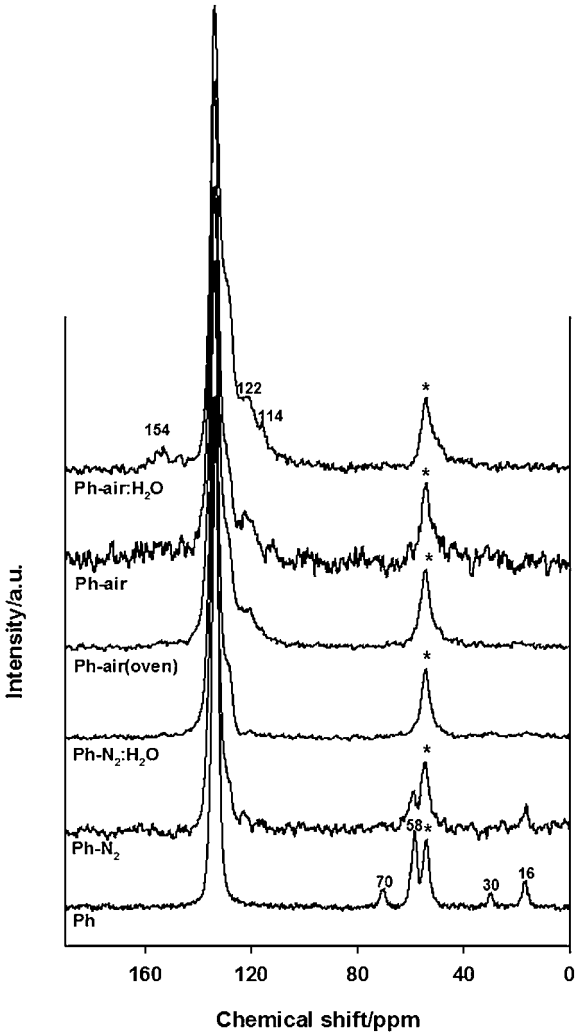

Fig. 8 ^{13}C CP/MAS NMR spectra of the extracted and calcined (up 400 °C) phenylene-bridged periodic mesoporous organosilicas.

were more easily affected by the thermal treatment. Thus, the decrease in the proportion of T^1, T^2 and T^3 sites between the samples Ph–N_2 and Ph-air : H_2O was 85%, 64% and 48%, respectively. Besides Q^2 and Q^3 sites, Q^4 units were generated by further condensation of silanol groups belonging to the other Q sites. In fact, the condensation degree was quite similar for all the hybrids (Table 3) which suggests that Si–C bonds were progressively replaced by Si–O–Si groups, that is, the Ph sample is being transformed from a PMOs to an anchored organosilica depending on the thermal treatment. Van der Voort *et al.*[65] studied the thermally induced metamorphosis in ethenylene-bridged PMOs (100% *trans*) and proposed that Si–C bond cleavage occurs by proton transfer from silanol groups to ethenylene bridging groups giving rise to terminal vinyl groups and siloxane bridges. However, the mechanism of Si–C bond cleavage for phenylene-bridged PMO should be different because it did not proceeded under N_2 unlike the ethenylene-bridged

Table 3 ^{29}Si MAS NMR results obtained for periodic mesoporous organosilicas

PMOs	T^1 (%)	T^2 (%)	T^3 (%)	Q^2 (%)	Q^3 (%)	Q^4 (%)	Condensation degree (%)	Molar ratio C*/Si[a]
Ph	13.4	56.7	29.9	—	—	—	72	1.00
Ph–N_2	18.0	48.9	33.1	—	—	—	>72	<1.00
Ph–N_2 : H_2O	16.2	38.6	32.4	4.0	6.8	2.0	73	0.86
Ph-air	9.4	28.3	29.0	7.8	12.8	12.7	77	0.66
Ph-air (oven)	4.4	27.8	25.5	5.0	25.9	11.4	79	0.63
Ph-air : H_2O	2.7	7.8	17.1	11.6	34.4	16.4	78	0.40

[a] C* represents a carbon atom attached to a silicon atom.

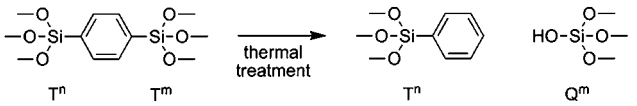

Scheme 1 Transformation of Si sites by cleavage of C–Si bonds after oxidative thermal treatments.

Table 4 Elemental compositions and C/Si atomic ratios for Ph–PMOs subjected to different thermal treatments

Sample	Si (wt%)	C (wt%)	C/Si ratio
Ph	22.56	34.91	3.60
Ph–N_2	24.12	33.73	3.26
Ph–N_2 : H_2O	25.79	32.10	2.91
Ph-air	23.64	28.56	2.83
Ph-air (oven)	26.52	26.01	2.29
Ph-air : H_2O	24.44	21.96	2.10

material. When the Ph material was calcined in the air at 600 and 800 °C, the ^{29}Si NMR spectra only exhibited the peaks corresponding to Q sites (see Fig. S4†).

The elemental analysis results for the different samples are shown in Table 4. As can be observed, the C/Si atomic ratios for the Ph and Ph–N_2 samples were 3.60 and 3.26, respectively, considerably higher than the calculated theoretical value 3.00 for the totally condensed structure ($Si_2C_6H_4O_3$), due to the presence of surfactant molecules and/or non-hydrolyzed ethoxy groups (both confirmed by ^{13}C NMR and DRIFT). However, Ph–N_2 : H_2O and Ph-air samples exhibited C/Si ratios slightly lower than 3.00, whereas Ph-air (oven) and Ph-air : H_2O materials showed values much lower, *i.e.* 2.29 and 2.10, respectively. Thus, the loss of organic matter from the hybrid materials with the thermal treatment followed the same order as the Q/T sites ratios. In fact, by comparing the C*/Si and C/Si ratios determined by ^{29}Si NMR and elemental analysis, respectively, for the different samples, it can be concluded that the Ph–N_2 and Ph–N_2 : H_2O samples suffer small changes upon calcination, whereas the Ph-air sample mainly undergoes cleavage of C–Si bonds and the Ph-air (oven) and particularly Ph-air : H_2O samples are subjected to an extensive C–Si bonds cleavage as well as an important decomposition of the phenylene bridges.

Sulfonic acid functionalized phenylene-bridged PMOs

After the phenylene-bridged PMOs were functionalized by reaction with chlorosulfonic acid, their structural and surface properties remained practically unchanged (Table 5 and Fig. S5†). Also, the NMR results suggested that additional degradation by bond cleavage or oxidation did not occurred (see Fig. S6, ESI†).

The amount of acid sites, *i.e.* sulfonic groups, for the functionalized PMOs varied in the range 0.27–0.75 mmol H^+ g^{-1}, depending on the previous calcination treatment. Thus, those materials with higher proportion of Q sites had the higher acidity. It could be explained by the cleavage of C–Si bonds which gave rise to monosubstituted phenyl rings, more reactive in the electrophilic aromatic substitution. These results are in agreement with those reported by Inagaki *et al.*[18] who obtained an acidity of 0.4 mmol H^+ g^{-1} for the non-calcined phenylene-bridged PMOs.

The sulfonated PMOs were used as catalysts for the esterification between acetic acid and ethanol. The phenylene-bridged PMO exhibited a very small activity similar to that of the blank reaction. Table 6 shows the reaction rate for the different sulfonated samples. As can be seen, all of them are more active than the non-sulfonated sample. Those materials obtained by sulfonation of PMOs calcined under air presented higher activity than those calcined under nitrogen, with the exception of the Ph-air–SO_3H sample. In general, the catalytic activity could be roughly correlated to the population of sulfonic groups. However, the Ph-air–SO_3H sample gave lower reaction rate than expected according to its acidity. This suggests the participation of other factors besides acidity in this reaction. Some possible factors could be diffusion, accessibility, polarity and chemical environment of the sulfonic groups, among others. The lack of a good correlation between the number of acid sites and the catalytic activity was also observed by Kapoor *et al.*[31,32] in Friedel–Crafts acylations. They found by comparing sulfonated PMOs with cubic and hexagonal symmetry that the former was more active due to the better accessibility to the active sites and

Table 6 Catalytic activities (reaction rates[a] and TOF[b]) of sulfonic acid functionalized mesoporous materials

Sample	Fresh catalysts[c]	Reuse[c]	Fresh catalysts[d]
Ph	21 (—)	—	—
Ph–N_2–SO_3H	36 (129)	—	13 (46)
Ph–N_2 : H_2O–SO_3H	28 (85)	—	9 (27)
Ph-air–SO_3H	23 (35)	—	14 (21)
Ph-air : H_2O–SO_3H	43 (57)	41 (55)	31 (41)
Ph-air (oven)–SO_3H	54 (84)	48 (75)	—
Amberlyst-15	93 (21)	91 (21)	21 (5)

[a] mmol h^{-1} g^{-1}. [b] h^{-1} (in brackets). [c] Reaction conditions: ethanol, 0.760 mol; acetic acid, 0.076 mol; catalyst, 0.15 g; and reaction temperature, 70 °C. [d] Reaction conditions: ethanol, 0.076 mol; acetic acid, 0.076 mol; water, 1.43 mol; catalyst, 0.15 g; and reaction temperature, 80 °C.

Table 5 Physicochemical properties of sulfonic acid functionalized phenylene-bridged PMOs[a]

Sample	*d*/Å	BET surface area/m^2 g^{-1}	Atomic ratio C/Si	Condensation degree (%)	Molar ratio C*/Si	Acidity/mmol H^+ g^{-1} [b]
Ph–N_2–SO_3H	51	843	3.16	70	<1.00	0.28
Ph–N_2 : H_2O–SO_3H	50	954	3.14	74	0.83	0.33
Ph-air–SO_3H	50	778	2.77	76	0.71	0.65
Ph-air (oven)–SO_3H	49	959	2.27	77	0.61	0.64
Ph-air : H_2O–SO_3H	49	740	1.85	75	0.40	0.75

[a] See Tables 2 to 4 for comparison. [b] Calculated by the titration method.

diffusion of reactants and products in this structure. All sulfonated PMOs gave a lower rate than a commercial Amberlyst-15 resin. However, due to the huge differences in acidity between the resin and the PMO materials, once calculated the catalytic activity per acid site (*i.e.*, the turnover frequency), all PMOs exhibited higher TOF than Amberlyst-15.

After the reaction, some sulfonated PMOs were recovered by filtration, washed and reused again in the esterification. As can be observed in Table 6, the lost of activity was low, similar to that of Amberlyst-15, what means that sulfonic acid groups were relatively stable and as a consequence these catalysts could be easily recycled, as observed also by other authors.[31,32]

Due to their high hydrophobicity, well-defined mesoporous structure and high stability in aqueous media, functionalized PMO materials look promising for their application as catalysts in water. Thus, some sulfonated phenylene-bridged PMOs were tested as catalysts for the esterification of acetic acid with ethanol by using water as solvent (Table 6). As can be observed, the activity of most of the PMOs is close to that of Amberlyst-15 and even higher in the case of the Ph-air : H_2O–SO_3H sample. Other authors have also reported the good performance of PMO materials grafted with propyl sulfonic acid groups in aqueous catalytic reactions.[66,67] After reactions, all catalysts preserved their structural and surface properties. Thus, the Ph-air : H_2O–SO_3H material had an exchange capacity of 0.71 mmol H^+ g^{-1}, very close to that of the fresh catalyst (Table 5), indicating the absence of sulfonic groups leaching during the catalytic tests.

Conclusions

Phenylene-bridged PMOs undergo structural and surface changes upon calcination under different conditions. Thus, while heating under nitrogen up to 400 °C has revealed no modifications of the material, the treatments under humid conditions and/or oxidizing atmosphere have led to C–Si bond cleavage and the generation of new surface functionalities which have been tentatively proposed as phenolic and carbonyl groups. Subsequent sulfonation of these materials with chlorosulfonic acid has not given rise to further changes. The formation of Si–Ph groups has made this treatment more effective on those materials subjected to calcination in air whose exchange capacity has been much higher than that for the others (0.7 *vs.* 0.4 mmol H^+ g^{-1}). Although other factors could have influenced the catalytic activity, in general those materials sulfonated more extensively have provided the higher reaction rate in the esterification of acetic acid with ethanol. As a consequence, an Amberlyst-15 resin which has been used for comparison has resulted to be more active under the same reaction conditions. However, when using water as solvent, a humid air-calcined phenylene-bridged PMO functionalized with sulfonic acid groups have been more active than Amberlyst-15, thus showing the promising application of these PMOs as catalysts in aqueous media.

Acknowledgements

The authors wish to acknowledge funding of this research by Ministerio de Ciencia e Innovación (Project MAT2010-18778) and Junta de Andalucía (Project P06-FQM-01741). D. E. thanks Ministerio de Educación y Ciencia of Spain for a research fellowship. Also, the authors thank Els De Canck for some nitrogen adsorption measurements.

References

1 C. T. Kresge, M. E. Leonowicz, W. J. Roth, J. C. Vartuli and J. S. Beck, *Nature*, 1992, **359**, 710.
2 J. S. Beck, J. C. Vartuli, W. J. Roth, M. E. Leonowicz, C. T. Kresge, K. D. Schmitt, T.-W. Chu, D. H. Olson, E. W. Sheppard, S. B. McCullen, J. B. Higgins and J. L. Schlenker, *J. Am. Chem. Soc.*, 1992, **114**, 10834.
3 X. Feng, G. E. Fryxell, L. Q. Wang, A. Y. Kim, J. Liu and K. M. Kemmer, *Science*, 1997, **276**, 923.
4 A. Stein, B. J. Melde and R. C. Schroden, *Adv. Mater.*, 2000, **12**, 1403.
5 S. L. Burkett, S. D. Sims and S. Mann, *Chem. Commun.*, 1996, 1367.
6 D. J. Macquairre, *Chem. Commun.*, 1996, 1961.
7 T. Asefa, M. J. MacLachlan, N. Coombs and G. A. Ozin, *Nature*, 1999, **402**, 867.
8 S. Inagaki, S. Guan, Y. Fukushima, T. Ohsuna and O. Terasaki, *J. Am. Chem. Soc.*, 1999, **121**, 9611.
9 B. J. Melde, B. T. Holland, C. F. Blanford and A. Stein, *Chem. Mater.*, 1999, **11**, 3302.
10 T. Asefa, M. J. MacLachlan, H. Grondey, N. Coombs and G. A. Ozin, *Angew. Chem., Int. Ed.*, 2000, **39**, 1808.
11 S. Guan, S. Inagaki, T. Ohsuna and O. Terasaki, *J. Am. Chem. Soc.*, 2000, **122**, 5660.
12 M. C. Burleigh, M. A. Markowitz, S. Jayasundera, M. S. Spector, C. W. Thomas and B. P. Gaber, *J. Phys. Chem. B*, 2003, **107**, 12628.
13 E.-B. Cho and K. Char, *Chem. Mater.*, 2004, **16**, 270.
14 K. Nakajima, D. Lu, J. N. Kondo, I. Tomita, S. Inagaki, M. Hara, S. Hayashi and K. Domen, *Chem. Lett.*, 2003, 950.
15 W. Wang, S. Xie, W. Zhou and A. Sayari, *Chem. Mater.*, 2004, **16**, 1756.
16 M. C. Burleigh, S. Jayasundera, C. W. Thomas, M. S. Spector, M. A. Markowitz and B. P. Gaber, *Colloid Polym. Sci.*, 2004, **282**, 728.
17 C. Yoshina-Ishii, T. Asefa, N. Coombs, M. J. MacLachlan and G. A. Ozin, *Chem. Commun.*, 1999, 2539.
18 S. Inagaki, S. Guan, T. Ohsuna and O. Terasaki, *Nature*, 2002, **416**, 304.
19 Y. Goto and S. Inagaki, *Chem. Commun.*, 2002, 2410.
20 Q. Yang, M. P. Kapoor and S. Inagaki, *J. Am. Chem. Soc.*, 2002, **124**, 9694.
21 M. P. Kapoor, S. Inagaki, S. Ikeda, K. Kakiuchi, M. Suda and T. Shimada, *J. Am. Chem. Soc.*, 2005, **127**, 8174.
22 A. Sayari and W. Wang, *J. Am. Chem. Soc.*, 2005, **127**, 12194.
23 M. P. Kapoor, Q. Yang and S. Inagaki, *J. Am. Chem. Soc.*, 2002, **124**, 15176.
24 K. Okamoto, Y. Goto and S. Inagaki, *J. Mater. Chem.*, 2005, **15**, 4136.
25 J. Morell, G. Woltner and M. Fröba, *Chem. Mater.*, 2005, **17**, 804.
26 E.-B. Cho and D. Kim, *Chem. Lett.*, 2007, 118.
27 M. Álvaro, M. Benítez, J. F. Cabeza, H. García and A. Leyva, *J. Phys. Chem. C*, 2007, **111**, 7532.
28 Y. Goto, N. Mizoshita, O. Ohtani, T. Okada, T. Shimada, T. Tani and S. Inagaki, *Chem. Mater.*, 2008, **20**, 4495.
29 Y. Goto, K. Nakajima, N. Mizoshita, M. Suda, N. Tonaka, T. Hasegawa, T. Shimada, T. Tani and S. Inagaki, *Microporous Mesoporous Mater.*, 2009, **117**, 535.
30 Y. Goto and S. Inagaki, *Microporous Mesoporous Mater.*, 2006, **89**, 103.
31 M. P. Kapoor, M. Yanagi, Y. Kasama, T. Yokoyama, S. Inagaki, T. Shimada, H. Nanbu and L. R. Juneja, *J. Mater. Chem.*, 2006, **16**, 3305.
32 M. P. Kapoor, M. Yanagi, Y. Kasama, T. Yokoyama, S. Inagaki, T. Shimada, H. Nanbu and L. R. Juneja, *Microporous Mesoporous Mater.*, 2007, **101**, 231.
33 W. Wang, W. Zhou and A. Sayari, *Chem. Mater.*, 2003, **15**, 4886.
34 M. P. Kapoor, Q. Yang and S. Inagaki, *Chem. Mater.*, 2004, **16**, 1209.
35 B. Onida, L. Borello, C. Busco, P. Ugliengo, Y. Goto, S. Inagaki and E. Garrone, *J. Phys. Chem. B*, 2005, **109**, 11961.
36 B. Onida, L. Borello, C. Busco, P. Ugliengo, Y. Goto, S. Inagaki and E. Garrone, *J. Phys. Chem. B*, 2005, **109**, 21732.

37 K. Okamoto, M. P. Kapoor and S. Inagaki, *Chem. Commun.*, 2005, 1423.
38 E.-B. Cho, D. Kim and M. Jaroniec, *Langmuir*, 2007, **23**, 11844.
39 H. Zhong, G. Zhu, J. Yang, P. Wang and Q. Yang, *Microporous Mesoporous Mater.*, 2007, **100**, 259.
40 Ö. Dag, C. Yoshina-Ishii, T. Asefa, M. J. MacLachlan, H. Grondey, N. Coombs and G. A. Ozin, *Adv. Funct. Mater.*, 2001, **11**, 213.
41 B. D. Hatton, K. Landskron, W. Whitnall, D. D. Perovic and G. A. Ozin, *Adv. Funct. Mater.*, 2005, **15**, 823.
42 O. Ohtani, Y. Goto, K. Okamoto and S. Inagaki, *Mater. Lett.*, 2006, **60**, 177.
43 S. Ito, S. Fukuya, T. Kusumi, Y. Ishibashi, H. Miyasaka, Y. Goto, M. Ikai, T. Tani and S. Inagaki, *J. Phys. Chem. C*, 2009, **113**, 11884.
44 Q. Yang, J. Liu, M. P. Kapoor, S. Inagaki and C. Li, *J. Catal.*, 2004, **228**, 265.
45 Q. Yang, M. P. Kapoor, S. Inagaki, N. Shirokura, J. N. Kondo and K. Domen, *J. Mol. Catal. A: Chem.*, 2005, **230**, 85.
46 Q. Yang, M. P. Kapoor, N. Shirokura, M. Ohashi, S. Inagaki, J. N. Kondo and K. Domen, *J. Mater. Chem.*, 2005, **15**, 666.
47 J. Liu, Q. Yang, M. P. Kapoor, N. Setoyama, S. Inagaki, J. Yang and L. Zhang, *J. Phys. Chem. B*, 2005, **109**, 12250.
48 J. A. Melero, R. van Grieken and G. Morales, *Chem. Rev.*, 2006, **106**, 3790.
49 B. Rác, P. Hegyes, P. Forgo and A. Molnár, *Appl. Catal., A*, 2006, **299**, 193.
50 C. Li, J. Yang, X. Shi, J. Liu and Q. Yang, *Microporous Mesoporous Mater.*, 2007, **98**, 220.
51 A. Karam, J. C. Alonso, T. I. Gerganova, P. Ferreira, N. Bion, J. Barrault and F. Jérome, *Chem. Commun.*, 2009, 7000.
52 K. Nakajima, I. Tomita, M. Hara, S. Hayashi, K. Domen and J. N. Kondo, *Adv. Mater.*, 2005, **17**, 1839.
53 D. Dubé, M. Rat, F. Béland and S. Kaliaguine, *Microporous Mesoporous Mater.*, 2008, **111**, 596.
54 B. S. Furniss, A. J. Hannaford, P. W. G. Smith and A. R. Tatchell, in *Vogel's Textbook of Practical Organic Chemistry*, ed. L. House, B. Mill and H. Essex, England, 5th edn, 1989, ch. 6, p. 873.
55 M. P. Kapoor, N. Setoyama, Q. Yang, M. Ohashi and S. Inagaki, *Langmuir*, 2005, **21**, 443.
56 L. Zhang, Q. Yang, W. Zhang, Y. Li, J. Yang, D. Jiang, G. Zhu and C. Li, *J. Mater. Chem.*, 2005, **15**, 2562.
57 X. Guo, X. Wang, H. Zhang, L. Fu, H. Guo, H. J. Yu, L. D. Carlos and K. Yang, *Microporous Mesoporous Mater.*, 2008, **116**, 28.
58 B. Camarota, B. Onida, Y. Goto, S. Inagaki and E. Garrone, *Langmuir*, 2007, **23**, 13164.
59 J. Robertson, *Mater. Sci. Eng., R*, 2002, **37**, 129.
60 F. Hoffmann, M. Güngerich, P. J. Klar and M. Fröba, *J. Phys. Chem. C*, 2007, **111**, 5648.
61 U. Díaz, T. García, A. Velty and A. Corma, *J. Mater. Chem.*, 2009, **19**, 5970.
62 D. Zhou, X. B. Luo, H. L. Zhang, C. Dong, Q. H. Xia, Z. M. Liu and F. Deng, *Microporous Mesoporous Mater.*, 2009, **121**, 194.
63 M. Kuroki, T. Asefa, W. Whitnal, M. Kruk, C. Yoshina-Ishii, M. Jaroniec and G. A. Ozin, *J. Am. Chem. Soc.*, 2000, **124**, 13886.
64 E. Pretsch, P. Bühlmann, C. Affolter, A. Herrera and R. Martínez, in *Determinación estructuralde compuestos orgánicos*, Springer-Verlag Ibérica, Barcelona, 2001, ch. 4, p. 97.
65 C. Vercaemst, J. T. Jones, Y. Z. Khimyak, J. C. Martins, F. Verpoort and P. Van der Voort, *Phys. Chem. Chem. Phys.*, 2008, **10**, 5349.
66 P. L. Dhepe, M. Ohashi, S. Inagaki, M. Ichikawa and A. Fukuoka, *Catal. Lett.*, 2005, **102**, 163.
67 A. Karam, J. C. Alonso, T. Ivanova, P. Ferreira, N. Bion, J. Barrault and F. Jérôme, *Chem. Commun.*, 2009, 7000.